Research Article

Journal of Physical Organic Chemistry

Received: 2 August 2007, Revised: 5 December 2007, Accepted: 7 December 2007, Published online in Wiley InterScience: 4 February 2008

(www.interscience.wiley.com) DOI 10.1002/poc.1318

Ring-chain interconversion of sulforhodamine-amine conjugates involves an unusually labile C—N bond and allows measurement of sulfonamide ionization kinetics

John E. T. Corrie[a]*, John F. Eccleston[a], Michael A. Ferenczi[a†], Madeleine H. Moore[b], Johan P. Turkenburg[b] and David R. Trentham[a]

pH-dependent interconversion between ring and chain forms of sultams/sulfonamides derived from conjugates of sulforhodamines with amines, and the associated sulfonamide ionization, have been studied by a combination of equilibrium and kinetic methods. The colorless, ring-closed sultam form is favored at alkaline pH with an apparent pK_a of 7.37 for the color change of the methylamine conjugate of Sulforhodamine B. The ring-closed form is also favored at very low pH (apparent p$K_a \sim 0.68$) by protonation of both diethylamino substituents. The kinetics of interconversion between open and closed forms were measured at 4°C over the pH range 0–13. The observed rate constant ranges over nine orders of magnitude from $4.8 \times 10^{-4}\,s^{-1}$ at pH 1 to $2.27 \times 10^{6}\,s^{-1}$ at pH ≥ 12. Above pH 2, the data are accommodated by a mechanism that includes cleavage of the sultam C—N bond in the ring opening step with a sulfonamide anion as the leaving group, and in the reverse reaction, OH^--dependent ionization of the sulfonamide at $4.8\ (\pm 2.0) \times 10^{9}\,M^{-1}\,s^{-1}$. Below pH 2, H^+-dependent protonation occurs at $1.4\ (\pm 0.4) \times 10^{-3}\,M^{-1}\,s^{-1}$. X-ray crystallography of a related *N*-methylsultam showed that the labile, endocyclic C—N bond is significantly longer than the exocyclic N—CH_3 bond (1.509 Å and 1.445 Å, respectively). Laser-induced ring opening of the closed form has potential application as an orientation probe of biological macromolecules. © Crown Copyright 2008. Reproduced with the permission of the Controller of HMSO. Published by John Wiley & Sons, Ltd.

Supplementary electronic material for this paper is available in Wiley InterScience at http://www.mrw.interscience. wiley.com/suppmat/0894-3230/suppmat/v20.html

Keywords: rhodamine; sultam; stopped-flow; flash photolysis; kinetics

INTRODUCTION

The fluorescence properties of rhodamine dyes, notably their absorption and emission in the visible spectrum, brightness and resistance to photobleaching, have been widely exploited in applications that range from dye lasers to interrogation of single molecules. Recent examples of advanced applications in biology include fluorescence polarization measurements on rhodamines attached to proteins to determine orientations and motions of protein domains *in situ* [1,2] or at the single molecule level,[3] and localization with nm-resolution of single rhodamines attached to proteins.[4] Any such studies are underpinned by knowledge of the underlying chemistry of the rhodamine probes. In the present work, we have investigated the kinetics of color changes in a sulforhodamine derivative that can be switched between colored (fluorescent) and colorless (non-fluorescent) forms in response to pH and can also be transiently converted from the colorless to colored form by laser pulse illumination with near-UV light. The latter property has potential for time-resolved optical polarization studies to extend previous work,[1–3] since flash illumination with a linearly polarized source would generate a fluorophore with an anisotropic distribution. Reversion to the colorless form takes place on a wide time scale, depending on the prevailing pH. *Inter alia* this process enables investigation of the kinetics of sulfonamide ionization, not previously studied among the extensive body of diffusion-controlled ionization reactions that are a topic of continued research interest.[5,6]

This paper is based on previous work in which the *mono*sulfonyl chloride derived from the widely used fluorescent dye Sulforhodamine B **1** was shown to exist in two isomeric forms

* *MRC National Institute for Medical Research, The Ridgeway, Mill Hill, London NW7 1AA, UK.*
E-mail: jcorrie@nimr.mrc.ac.uk

a *J. E. T. Corrie, J. F. Eccleston, M. A. Ferenczi, D. R. Trentham*
MRC National Institute for Medical Research, The Ridgeway, Mill Hill, London NW7 1AA, UK

b *M. H. Moore, J. P. Turkenburg*
York Structural Biology Laboratory, Department of Chemistry, University of York, Heslington, York YO1 5DD, UK

† *National Heart and Lung Institute, Imperial College London, Sir Alexander Fleming Building, London SW7 2AZ, UK*

Journal of Physical Organic Chemistry

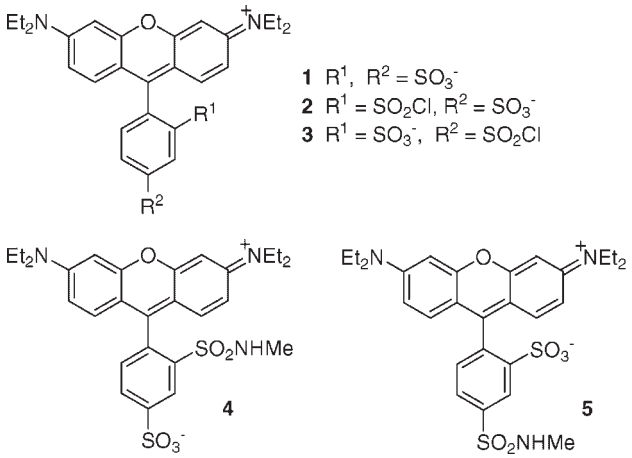

Figure 1. Structures of compounds **1**–**5**

2 and **3**.[7] We also showed that isomer **2**, with a sulfonyl chloride *ortho* to the xanthylium system, reacts with methylamine to form a sulfonamide **4** that undergoes pH-dependent reversible cyclization to a colorless spirosultam (Scheme 1). The color of the isomeric sulfonamide **5** derived from **3** was unaffected by pH except at high acidity (≤pH 1; see below). The colorless, spirosultam form of **4** was favored at alkaline pH and the apparent pK_a for the interconversion was 7.37, determined from absorbance measurements at 567 nm in 25% ethanol–75% aqueous buffer (v/v). The water–ethanol solvent is unlikely to cause a pH shift of more than 0.1 unit from the value in water.[8] Concentrations of the sultam were not reliable without this amount of ethanol, presumably because of losses by adsorption of the more hydrophobic ring-closed form of the dye onto surfaces.

The kinetics of the ring-chain interconversion outlined in Scheme 1 had been briefly examined in stopped-flow experiments by imposing rapid pH changes to solutions of **4**.[7] The observed rate constant of the absorbance change, k_{obs}, was ~200 s^{-1} (4°C) near pH 7, whether approached from alkaline or acidic starting conditions. The present paper reports the detailed kinetics of this process over the pH range 0–13. Across this range, k_{obs} varies more than nine orders of magnitude. The reaction involves multiple protonation states and we present a scheme that fits the experimental data. Various supporting data were used in developing the mechanism including results from X-ray crystallography of a model sultam to help rationalize the unusually facile C—N bond cleavage that occurs in the ring-opening step.

RESULTS

The data described below were obtained on samples of different compositions. In our initial work we used a mixture of the isomeric compounds **4** and **5** (ratio ~2.6:1) and this mixture was also used for all the pH-jump kinetic studies reported here. In work on equilibrium measurements across the pH range, and on photolytic ring opening of the colorless form of **4** at alkaline pH, it became necessary to use a purified sample of **4** that was obtained as previously described[7] by extensive chromatography of the **4** and **5** mixed isomers (Fig. 1)

Figure 2 shows a titration of pure **4** over the pH range 0–10 that extends previous data[7] by revealing a second titration with

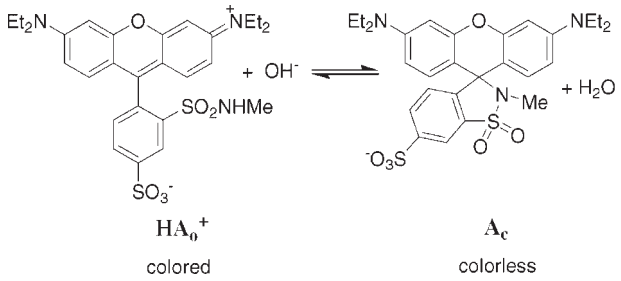

Scheme 1. Overall ring-chain interconversion of sulforhodamine-amine conjugates

apparent pK_a ~0.68. The titration at this low pH evidently results from protonation of both diethylamino groups (see below). This pK_a value, which derives from a fit to data collected over a wider pH range and with many more experimental points than shown in Fig. 2, is approximate because of probable errors in pH measured with the glass electrode at high acidity (see Supplementary Information, Fig. S1, for details of the fit and discussion of the deviation of the fitted line from the data points). The kinetics of the color changes associated with both pK_a values were determined here to develop a mechanistic scheme for the processes.

Observed rate constants (k_{obs}) for color changes of **4** in either direction over the pH range 2.1–7.4 were measured in stopped-flow experiments by mixing solutions of the mixed isomers **4** and **5** at pH 4 or 9 with buffers at various pH values and recording absorbance changes at 567 nm. All solutions contained 25% ethanol (by volume), as noted above. The stopped-flow measurements were made at 4°C to bring the fastest rates into an observable range, and all subsequent kinetic measurements were therefore made at the same temperature. Typical stopped-flow absorbance records are shown in Fig. 2A and B for ring opening and ring closing, respectively. The data were well fitted by single exponentials and Table 1 shows values of k_{obs} across this pH range. Near pH 7 it was possible to monitor reactions starting from either pH 4 or pH 9, and values of k_{obs} in this region were independent of the direction of the pH change, indicating that the same species were undergoing equilibration in the two cases.

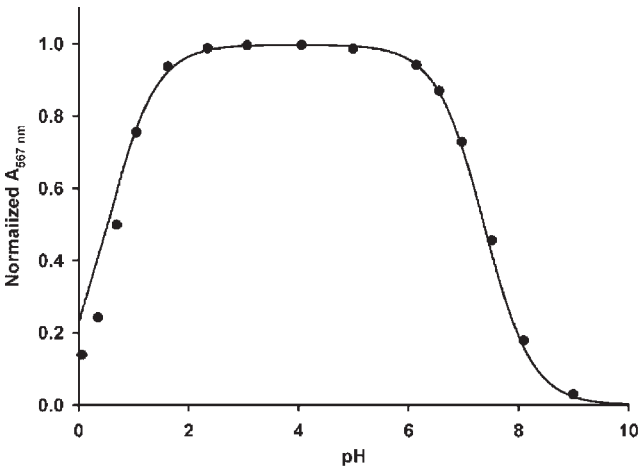

Figure 2. Absorbance values of **4** at 567 nm, normalized to the value at pH 4.0, are shown as the solid circles. The line is that of the modeled proportion of the colored form across the pH range (see the Eqn (17) in the 'Discussion' Section)

Table 1. Observed rate constants, k_{obs}, for stopped-flow pH shift experiments

Final pH	Initial pH	Mixing buffer (pH)	Absorbance change	k_{obs} (s^{-1})[a]	k_{obs}' (s^{-1})[b]
2.14	9.0	Citrate (2.0)	+	0.021 ± 0.001	0.021
2.55	9.0	Citrate (2.5)	+	0.19 ± 0.02	0.19
3.03	9.0	Citrate (3.0)	+	1.3 ± 0.2	1.3
3.45	9.0	Citrate (3.5)	+	4.4 ± 0.3	4.4
4.00	9.0	Citrate (4.0)	+	19.7 ± 0.9	19.7
4.56	9.0	Citrate (4.5)	+	51.3 ± 3.5	51.3
5.06	9.0	Citrate (5.0)	+	95.1 ± 6.6	95.1
5.56	9.0	Citrate (5.5)	+	120 ± 3	118
6.11	9.0	Citrate (6.0)	+	118 ± 3	112
6.57	9.0	MES (6.5)	+	158 ± 5	141
6.83	4.0	MOPS (7.0)	−	180 ± 33	150
7.03	9.0	MOPS (7.0)	+	217 ± 8	169
7.36	4.0	MOPS (7.5)	−	245 ± 22	143

[a] Values are the means (±SD) of at least four determinations.
[b] $k_{obs}' = k_{obs}$ in the range pH 2.14–5.06 and modified for pH 5.56–7.36 (as shown in the 'Discussion' Section for details of this modification).

The rates of the color change at high acidity were measured by manual mixing of solutions of the **4** and **5** mixture at pH 3 with different concentrations of hydrochloric acid. The loss of color was biphasic, comprising a rapid phase within the manual mixing time followed by a much slower process, as shown in Fig. 3C. As indicated in Fig. 2, the amplitude of this slow decolorization became greater as the acid concentration increased. Control experiments showed that Sulforhodamine B **1** also underwent a titration at low pH values, as shown by loss of color, but the full extent of this change occurred within the mixing time. Isomer **5** is expected to show similar behavior. Previous studies of other rhodamines,[9–12] including a very brief study of Sulforhodamine B,[12] have reported formation at low pH of doubly protonated species that have little absorption above ~550 nm and a new absorption band, maximal at ~500 nm but an order of magnitude less intense than the usual rhodamine absorption. Thus the rapid phase of decolorization when the **4** and **5** mixture was acidified is attributed to **5**. The slow phase was ascribed solely to isomer **4** and values of k_{obs} for this exponential process are given in Table 2. A control experiment with pure **4** showed only the slow phase of decolorization, in agreement with expectations from the argument presented above. The absorption spectrum, recorded in 2 M HCl, of the species formed by the slow decolorization process is shown in supplementary information (Fig. S2). In a further control experiment, an aliquot of the decolorized solution of pure **4** was diluted into a high molarity buffer at pH 4. The 567 nm absorption recorded as a function of time recovered within the mixing time to the value expected for the initial rhodamine concentration (i.e. after correction for the dilution factor) confirming that the decolorization process was quantitatively reversible.

At pH values above 7.4, the ring-closing reaction became too fast to follow by stopped-flow measurements and we adopted the reversible photolytic ring opening previously described by Gleiter and colleagues for related rhodamine lactams and sultams.[13,14] This achieves rapid generation of the open form, reclosure of which can be observed by monitoring the decay of its visible absorption. As the reaction requires **4** to be present in its colorless, closed form prior to photolysis, measurements were possible only at pH values above the apparent pK_a for ring closure. Thus, absorption records at 547 nm and 567 nm following 308 nm laser flash irradiation of **4** were obtained in the pH range 7.5–13. Over this range there was an absorption increase within the 30 ns laser pulse that was ascribed to ring opening of the colorless, closed form of **4**, followed by decay to starting material. Unlike the single exponential transients described above for the pH jump experiments, the decays observed in these photolysis experiments were generally biphasic so Scheme 1 was expanded to Scheme 2, a two-step reaction. The laser flash caused photogeneration of $\mathbf{A_o}$ from $\mathbf{A_c}$. However, over the pH range studied, at least three other transient phases not described by Scheme 2 were observed and these additional processes are discussed below.

Records of the absorption decays at 547 nm assigned to the two processes of Scheme 2, together with additional transients, are shown in Fig. 4 at selected pH values. Rate constants k_{fast}, k_{obs}, and k_{slow} and their associated absorption amplitude changes (Abs_1, Abs_2, and Abs_3, respectively) calculated from data recorded at intervals of 0.5 pH units are listed in Table 3. The process shown in Fig. 4A (pH 9.52) is assigned below to the slower (k_{obs}) component of the biphasic transient implicit in Scheme 2, while Fig. 4B shows the faster (k_{fast}) component at the same pH. Note that Abs_1 data associated with k_{fast} were each increased by 0.015 absorbance units (shown in 'Experimental' Section) to allow for reaction occurring between the peak of the laser flash and the point defined as time 'zero', at which the transient was at its maximum amplitude. This perturbation, caused by the laser flash, is evident in Fig. 4B as the negative signal during the ~100 ns prior to time zero. The main panel of Fig. 4C shows a record at pH 13.05 that is biphasic. The principal component has an exponential decay rate of $2.34 \times 10^6\ s^{-1}$, with a further component (22% amplitude of the overall transient) that was an order of magnitude slower. The theory developed below suggests that the transient at this high pH value should be a single exponential and the presence of the slower transient is unexpected. Traces recorded at pH 13 in the range 547–587 nm indicated that both

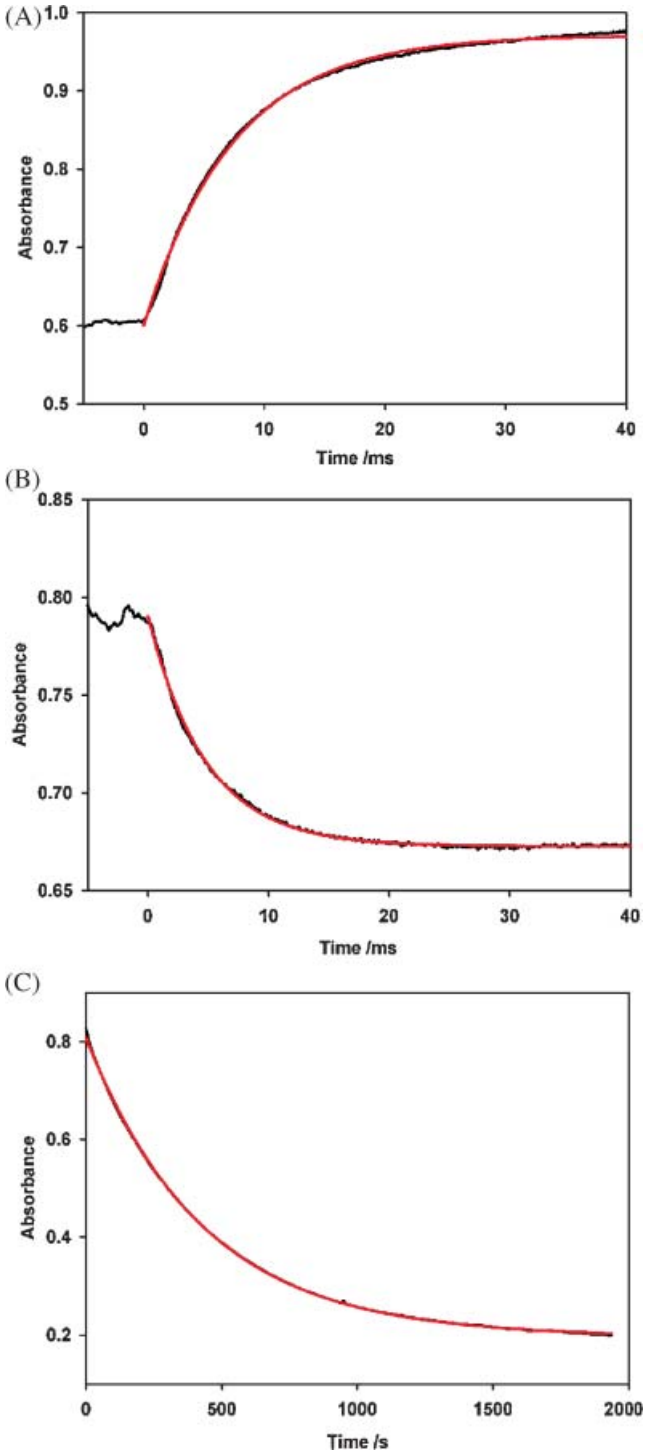

Figure 3. Kinetics of the 567 nm absorption of **4** (containing 28% of the total rhodamines as **5**) in response to pH changes. A: Stopped-flow spectrophotometric record from pH 9.0 to 6.57. B: Stopped-flow spectrophotometric record from pH 4.0 to 7.36. C: Manual-mixing spectrophotometric record from pH 3.0 to 0.0. This record does not show the fast drop of ~0.29 absorbance units that occurs upon mixing through partial protonation of **5** (as discussed in the text). In each panel the data are overlaid with the best-fit single exponential line in red.

Table 2. Observed rate constants, k_{obs}, for manual mixing pH shift experiments

Final pH	$10^4 k_{obs}$ (s^{-1})	$10^4 k^*_{obs}$ (s^{-1})[c]
0.0	23[a]	23
0.3	9.7[b]	9.6
0.7	5.2[b]	4.8
1.0	4.8[a]	3.2

[a] Mean of two determinations.
[b] Single determination.
[c] k^*_{obs} is modified k_{obs} (as shown in the 'Discussion' Section for details of this modification).

transient species had the same spectrum, since the relative amplitude of the two phases was unaltered. Both transient processes probably reflect return to the closed form of **4** from its open form. While the faster process is postulated to occur as a result of Scheme 2, the origin of the slower process is unclear. Neither its amplitude nor its rate was affected by deoxygenation of the solution with a nitrogen purge and it was not investigated further.

The inset to Fig. 4C also shows that, at 567 nm, the instantaneous absorption increase at the time of the laser pulse was followed by a further increase ($t_{½}$ ~100 ns), with an amplitude at 567 nm that was ~20% of the instantaneous increase. The spectrum of the 100 ns transient was investigated by recording transients over the range 547–587 nm. This 100 ns transient was present at 587 nm but was not seen at 547 nm, though it may distort the tail of the instantaneous increase. The mechanism that gives rise to this transient was not pursued further. To obtain transients for absorption decays with minimal interference from the rising 100 ns transient, all data for quantitative mechanistic interpretation over the pH range 8.48–13.05 were obtained at 547 nm (Table 3). Transients associated with k_{obs}, when recorded at 547 nm, were about 50% lower in amplitude than at 567 nm. However, those associated with k_{fast} when recorded at 567 nm were either obscured by the 100 ns transient or difficult to quantify.

The process shown in the main panel of Fig. 4D (pH 8.04) is also assigned to the slower (k_{obs}) component of the biphasic transient implicit in Scheme 2. However, in this experiment and that at pH 7.52, significant fractions of **4** exist in the open form (41% at pH 7.52 and 18% at pH 8.04). The traces at these pH values show recoveries after the light flash to absorbance values below the pre-flash level followed by an exponential return to the initial baseline (40 s^{-1} at both pH values). These slow transients, exemplified in the inset panel of Fig. 4D, were absent at higher pH

$$HA_o^+ + OH^- \underset{k_{-1}'}{\overset{k_1'}{\rightleftharpoons}} H_2O + A_o \underset{k_o}{\overset{k_c}{\rightleftharpoons}} A_c$$

Scheme 2. Two-step mechanism for equilibration of the sultam **4** between its open and closed forms. HA_o^+ and A_c are as defined in Scheme 1 and A_o is the sulfonamide anion. See also the legend to Scheme 3 for structural definitions of these and related abbreviations

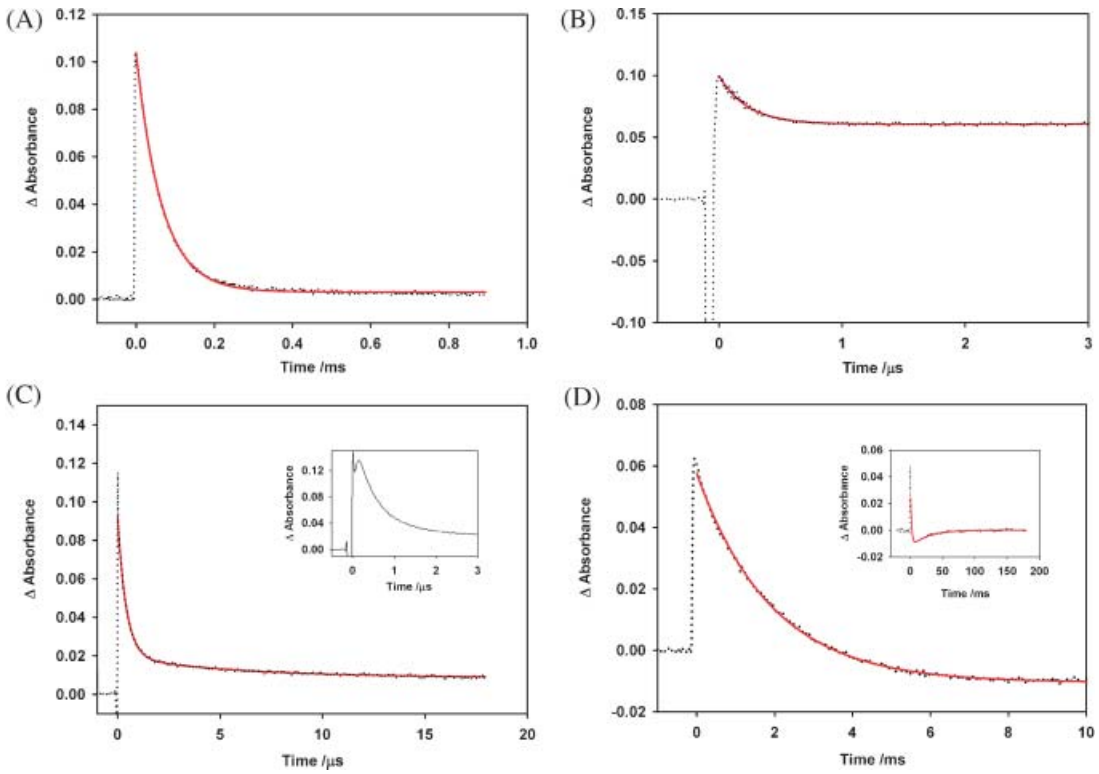

Figure 4. Kinetics of the absorption change of **4** following laser pulse irradiation. A,B: Records at 547 nm and pH 9.52 at two time scales. C: Record at 547 nm and pH 13.05 (the inset is a record at 567 nm and pH 12.99 that shows the rising 100 ns transient described in the text). D and its inset: Records at 567 nm and pH 8.04 at two time scales. In each panel data are overlaid with a best-fit single or double exponential line in red (shown in 'Experimental' Methods for details).

values where the proportion of the open form was insignificant. The 40 s^{-1} transient, whose origin is considered in the 'Discussion', is evidently associated with light absorption by the open form (i.e. HA_o^+) and this was briefly investigated. Thus, 308 nm laser flash illumination of Sulforhodamine B **1** gave a bi-exponential transient (relative increasing absorption amplitudes 0.65:1) with rate constants of ~10^4 and 2500 s^{-1} at pH 8 and 4°C. Sultam **4** at pH 4, where it exists entirely as HA_o^+, also showed a biphasic transient (relative increasing absorption amplitudes 1.4:1) with rate constants of ~2500 and 180 s^{-1}. It seems likely that light absorbed by the fraction of **4** existing as HA_o^+ at pH 7.5 and 8 gives rise to similar biphasic transients in which the faster phase is in the region of 2500 s^{-1}, while the slower phase is that shown in the inset of Fig. 4D. In quantitative terms Abs_2 (−0.073) at pH 8.04 (Fig. 4D) would have been reduced by about 20% if the same biphasic transient seen

Table 3. Effect of pH on photochemical kinetic and amplitude data for **4** at 547 nm

pH	$10^{-6}k_{fast}$ s^{-1} (Abs_1)	k_{obs} s^{-1} (Abs_2)	k_{slow} s^{-1} (Abs_3)
7.52[a]		297 (−0.034)	40 (0.022)
8.04[a]		498 (−0.073)	40 (0.010)
8.48	6.35 (−0.061)	1140 (−0.040)	
9.02	4.80 (−0.051)	6390 (−0.046)	
9.52	4.47 (−0.046)	15 300 (−0.047)	
10.03	3.13 (−0.078)	45 300 (−0.096)	
10.52	2.58 (−0.078)	1.20×10^5 (−0.078)	
10.99		2.67×10^6 (−0.072)	2.4×10^5 (−0.071)
11.50		1.85×10^6 (−0.089)	3.0×10^5 (−0.061)
11.99		2.21×10^6 (−0.043)	2.3×10^5 (−0.021)
12.50		2.21×10^6 (−0.081)	1.8×10^5 (−0.027)
13.05		2.34×10^6 (−0.090)	1.7×10^5 (−0.026)

[a] Data at pH 7.52 and 8.04 were collected at 567 nm.

Journal of Physical Organic Chemistry

for $H\mathbf{A_o}^+$ at pH 4 were present at pH 8.04. Because of this effect and the resultant uncertainty, data at pH 7.52 and 8.04 were not used in determining the rate constants of Scheme 2, although they were later checked for consistency with those rate constants (see the 'Discussion' section).

To summarize the laser pulse photochemical experiments, data relevant to interpreting the rate constants of Scheme 2 are listed as k_{fast} and k_{obs} in Table 3. Data for k_{slow}, for which illustrative examples are shown in Fig. 4C and the inset to Fig. 4D, were not used in this analysis, nor were the 100 ns transients illustrated by the inset to Fig. 4C.

In developing a mechanistic understanding of these processes, it was important to know whether there was a detectable amount of the open form of **4** at high pH. At pH 12 the absorbance of **4** was ~0.016% of that at pH 4 (measured absorbance values are given in the 'Experimental' Section). The peak of this very weak absorption was shifted to ~555 nm by spectral distortion from overlap with the tail of the near-UV absorption of the closed form of **4** that extends beyond 550 nm. The calculated contribution to the 567 nm absorbance at pH 12 based on the pK_a value of 7.37 for equilibrium of the open and closed forms is only 0.0023% of that at its maximal value, that is at pH 4. It follows that there is evidence for an additional colored species present at a level of ~0.014% in equilibrium with the closed form. In the mechanistic scheme developed below, this is assigned to the sulfonamide anion of **4** in its open form ($\mathbf{A_o}$ in Schemes 2 and 3).

As discussed below, this ring-chain interconversion involves an unusually facile C—N bond heterolysis and the lability of the endocyclic C—N bond in sultam **4** would be expected to have a structural basis in this and related compounds. To investigate this, the crystal structure of a model rhodamine sultam was determined. The known[15] sulforhodamine **6** was converted *via* its sulfonyl chloride to the colorless crystalline sultam **7** that also exhibited ring-chain interconversion (Fig. 5). Visible absorption spectra measured in aqueous ethanol buffers qualitatively confirmed the reversible color change but the closed form was too insoluble to allow reliable kinetic measurements to be performed. The X-ray structure (Fig. 6) confirmed the cyclic nature of **7** and showed significant differences between the two C—N bonds of the sultam moiety, with exocyclic and endocyclic C—N bond lengths of 1.445 Å and 1.509 Å, respectively. The implication of this bond extension is considered in the 'Discussion' Section.

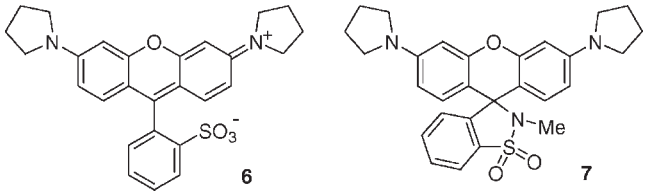

Figure 5. Structures of compounds **6** and **7**

DISCUSSION

Theory of photochemically induced and stopped-flow transients

Scheme 2 can be expressed in the form of a three-state system that has an analytical solution[16–18] describing time courses of formation and/or decay of $H\mathbf{A_o}^+$, $\mathbf{A_o}$, and $\mathbf{A_c}$.

$$H\mathbf{A_o}^+ \underset{k'_{-1}}{\overset{k'_1[OH^-]}{\rightleftharpoons}} \mathbf{A_o} \underset{k_o}{\overset{k_c}{\rightleftharpoons}} \mathbf{A_c} \qquad (1)$$

Note that k_o in Eqn (1) refers to the thermal ring-opening process, not the instantaneous photochemical opening that proceeds from an excited state. Following perturbation of the system from equilibrium, the time course of $[H\mathbf{A_o}^+]$ takes the form:

$$[H\mathbf{A_o}^+] = [H\mathbf{A_o}^+]_\infty - \alpha_1 \exp(-\lambda_1 t) - \alpha_2 \exp(-\lambda_2 t) \qquad (2)$$

Time courses of $[\mathbf{A_o}]$ and $[\mathbf{A_c}]$ take the same form with identical λ_1 and λ_2 but with constants $[H\mathbf{A_o}^+]_\infty$, α_1, and α_2 being replaced

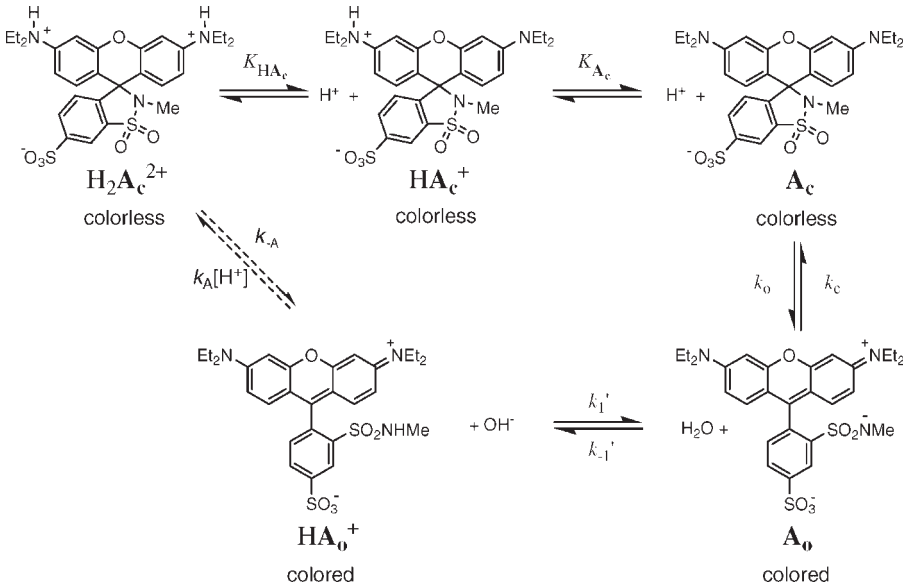

Scheme 3. Mechanism for interconversion of the colored and colorless forms of the rhodamine conjugate **4**. Abbreviations for the various species correspond to those used in the text. In denoting the charge on each species (e.g. $H_2\mathbf{A_c}^{2+}$), the negative charge of the sulfonate group present throughout has been ignored

J. Phys. Org. Chem. **2008**, 21 286–298 www.interscience.wiley.com/journal/poc

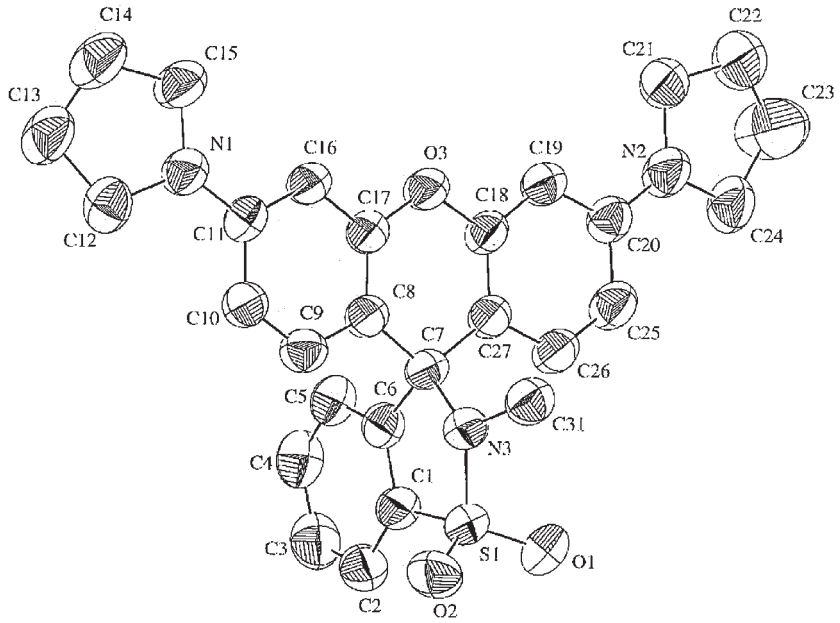

Figure 6. ORTEP diagram with 50% ellipsoids of the crystal structure of sultam **7**

by constants specific to [$\mathbf{A_o}$] and [$\mathbf{A_c}$]. λ_1 and λ_2 are the roots of Eqn (3).

$$\lambda_2 - (k'_1[OH^-] + k'_{-1} + k_c + k_o)\lambda + (k'_1k_c[OH^-] + k'_1k_o[OH^-] + k'_{-1}k_o) = 0 \quad (3)$$

It is evident that k_c must be much greater than k_o because the overall pK_a of 7.37 for H$\mathbf{A_o^+}$ to $\mathbf{A_c}$ is 4 units less than that for a typical sulfonamide. This inference is borne out by the spectral data that indicate the presence of a colored species at pH 12 ($\mathbf{A_o}$ according to Scheme 2) at a concentration ~0.014% that of $\mathbf{A_c}$. From the point of view of the kinetic analysis of the photochemical data at pH ≥ 8.48 (Table 3) it is therefore possible to treat the $\mathbf{A_o}$ to $\mathbf{A_c}$ transformation as irreversible. Expressions for λ_1 and λ_2 can be simplified to the following equations (see Reference[17], p. 313).

$$\lambda_1 = {}^1/_2\left\{k'_1[OH^-] + k'_{-1} + k_c + \left((k'_1[OH^-] + k'_{-1} + k_c)^2 - 4k'_1k_c[OH^-]\right)^{\frac{1}{2}}\right\} \quad (4)$$

$$\text{and } \lambda_2 = {}^1/_2\left\{k'_1[OH^-] + k'_{-1} + k_c - \left((k'_1[OH^-] + k'_{-1} + k_c)^2 - 4k'_1k_c[OH^-]\right)^{\frac{1}{2}}\right\} \quad (5)$$

We now consider Abs_t, the visible light absorption at time t after the laser pulse, expressed in Eqn (6) in terms of the absorption of each phase Abs_1 and Abs_2 (also observed experimentally, see below), and how it relates to [H$\mathbf{A_o^+}$] and [$\mathbf{A_o}$].

$$Abs_t = Abs_1 \exp(-\lambda_1 t) + Abs_2 \exp(-\lambda_2 t) \quad (6)$$

where Abs_1 and Abs_2 are absorptions of the two phases immediately following the laser flash. The species generated by photolysis and present at the instant after the laser pulse is the sulfonamide anion $\mathbf{A_o}$. The dark reactions that follow involve formation and decay of H$\mathbf{A_o^+}$ and formation of $\mathbf{A_c}$, and the observed absorption transient reflects changes in [H$\mathbf{A_o^+}$] and [$\mathbf{A_o}$].

We assume that the extinction coefficients of H$\mathbf{A_o^+}$ and $\mathbf{A_o}$ are the same and that $\mathbf{A_c}$ has insignificant visible light absorption at these wavelengths. Abs_t is then proportional to ([H$\mathbf{A_o^+}$] + [$\mathbf{A_o}$]). At the end of the transient [$\mathbf{A_o}$] is close to zero, as is [H$\mathbf{A_o^+}$] (except for measurements at pH 7.5 and 8 which are not used in the photochemical data analysis). At time zero (i.e. immediately after the laser pulse) [H$\mathbf{A_o^+}$] = [$\mathbf{A_c}$] = 0. In the analysis we consider only the fraction of $\mathbf{A_c}$ that undergoes ring opening. Likewise [H$\mathbf{A_o^+}$]$_\infty$ = [$\mathbf{A_o}$]$_\infty$ = 0, where the subscript denotes the end of the transient. In addition, [$\mathbf{A_o}$] at time zero equals [$\mathbf{A_c}$]$_\infty$. It follows (from Eqn (13) in Reference [18] where $Abs_1/Abs_2 = F_r$ etc.) that the absorption ratio of the two phases is

$$\frac{Abs_1}{Abs_2} = \frac{(k_c - \lambda_2)}{(\lambda_1 - k_c)} \quad (7)$$

The stopped-flow data above pH 5.5 in Table 1 can also be analyzed in terms of Eqn (1) using a similar formalism. Data below pH 5.5 are treated separately because pre-equilibrium protonation of the diethylamino groups in $\mathbf{A_c}$ perturbs the observed rate of ring opening (see below). After mixing solutions at pH 4 or 9 to a new pH in the range 5.5–7.36, the observed absorption change, ΔAbs, is proportional to change in [H$\mathbf{A_o^+}$]. Kinetic analysis is simplified to a single exponential response according to Eqn (8), since the steady-state approximation[19] applies in this pH range because [$\mathbf{A_o}$] ≪ [H$\mathbf{A_o^+}$] in the ms time domain (in practice k'_{-1} and $k_c \gg k'_1[OH^-]$ and k_o). Thus

$$\Delta Abs_t = \Delta Abs_T\left\{1 - \exp\left[-(k'_1k_c[OH^-] + k'_{-1}k_o)(k'_{-1} + k_c)^{-1}t\right]\right\} \quad (8)$$

where ΔAbs_t is the absorbance with respect to time and ΔAbs_T is the overall absorption change. The Δ notation is used because the extent of the absorbance change is dependent on the final pH in accord with the titration shown in Fig. 2. In the photochemical experiments under conditions where $k'_1[OH^-] \ll k'_{-1}$ and k_c [i.e. at pH 10.52 and below, where $k_{obs} \ll k_{fast}$ (Table 3)] the steady-state approximation also applies and hence the exponent term of Eqn (8) is also a valid route to determining k'_1.

Mechanism of the ring-chain interconversion

Scheme 3, which gives structures and defines the related abbreviations ($H_2\mathbf{A}_\mathbf{c}^{2+}$ etc.) for each of the species involved, shows a mechanism consistent with the equilibrium and kinetic data obtained for the interconversion of sultam **4** between its open and closed forms. At its heart, sulfonamide ionization is coupled to ring closure and the accompanying optical change provides a means to measure the kinetics of sulfonamide ionization. Data over the pH range 2–13 indicate that hydroxide ion dependent ionization (Eqn (9)) is an integral component of Scheme 3, as already implied by Scheme 2.

$$H\mathbf{A}_\mathbf{o}^+ + OH^- \underset{k'_{-1}}{\overset{k'_1}{\rightleftharpoons}} \mathbf{A}_\mathbf{o} + H_2O \qquad (9)$$

However, the kinetics of sulfonamide ionization need to be considered in terms of Eqn (10) as well as Eqn (9).

$$H\mathbf{A}_\mathbf{o}^+ \underset{k^*_{-1}}{\overset{k^*_1}{\rightleftharpoons}} \mathbf{A}_\mathbf{o} + H^+ \qquad (10)$$

Equations (9) and (10) allow for kinetic analysis as formulated by Eigen[5] of this proton transfer reaction over the entire pH range, where rate constants for deprotonation of $H\mathbf{A}_\mathbf{o}^+$ (k_1) and protonation of $\mathbf{A}_\mathbf{o}$ (k_{-1}) are expressed as:

$$k_1 = k'_1[OH^-] + k^*_1 \qquad (11)$$

and

$$k_{-1} = k'_{-1} + k^*_{-1}[H^+] \qquad (12)$$

We show below that the data over the pH range 2–13 indicate, as implied in Scheme 2, that Eqn (9) is an integral component of Scheme 3. However the dependence of k_{obs} on $[H^+]$ below pH 1 suggests Eqn (9) is no longer the pathway. Either a more direct pathway for the $H\mathbf{A}_\mathbf{o}^+$ to $H_2\mathbf{A}_\mathbf{c}^{2+}$ transition operates, as implied by the dashed arrows of Scheme 3 or possibly a pathway through $\mathbf{A}_\mathbf{o}$ as implied by Eqn (10). Which of these alternatives is the more likely is discussed below.

Data evaluation

To extract individual rate constants from the data, we first considered the photochemical results (Table 3), where the laser flash converts a fraction of $\mathbf{A}_\mathbf{c}$ into $\mathbf{A}_\mathbf{o}$.[13,14] Scheme 2 implies that $\mathbf{A}_\mathbf{o}$ is then subject to competing reactions, namely ring closure back to $\mathbf{A}_\mathbf{c}$ and H_2O-mediated protonation to $H\mathbf{A}_\mathbf{o}^+$ followed by flux back through $\mathbf{A}_\mathbf{o}$ to $\mathbf{A}_\mathbf{c}$. Over most of the pH range this gives rise to biphasic transients that are well resolved up to pH 10.5. However, above the pK_a of the sulfonamide (expected value ~11.5 from literature data[20]) little $H\mathbf{A}_\mathbf{o}^+$ is formed and a single exponential phase predominates, ascribed to the decay of $\mathbf{A}_\mathbf{o}$ to $\mathbf{A}_\mathbf{c}$ and controlled by k_c. (Note also in Eqn (5) that λ_2 tends to k_c when $k'_1[OH^-] \gg k'_{-1}$). Averaged k_{obs} values from the pH 12.50 and 13.05 data (Table 3) give $k_c = 2.27 \times 10^6\ s^{-1}$.

We next determined the kinetics of sulfonamide ionization, initially by data analysis from the pH range 8.48–10.52. In this range $k'_1[OH^-] \ll k'_{-1}$ so, from Eqn (4), λ_1 tends to $(k'_{-1} + k_c)$. Averaged k_{fast} values (Table 3) thus give $(k'_{-1} + k_c) = 4.27\ (\pm 1.48) \times 10^6\ s^{-1}$. Since $k_c = 2.27 \times 10^6\ s^{-1}$, the kinetic estimate is $k'_{-1} = 2.00\ (\pm 1.48) \times 10^6\ s^{-1}$. Note that we have used an average value of k_{fast}, whereas in fact k_{fast} decreases 2.6-fold over the 100-fold $[OH^-]$ range (Table 3). Other data (not shown) indicate a similar scatter of k_{fast} in the pH range of 8.48–10.52 but without the decreasing trend as $[OH^-]$ increased. Therefore k_{fast} has been treated as independent of $[OH^-]$ in this pH range.

A second estimate of k'_{-1} comes from consideration of the relative amplitude of the two phases in the pH range 8.48–10.52. From Table 3, $Abs_1 = -0.063\ (\pm 0.015)$ and $Abs_2 = -0.061\ (\pm 0.024)$. From Eqn (7), $Abs_1/Abs_2 = (k_c - \lambda_2)/(\lambda_1 - k_c) = k_c/k'_{-1}$, since λ_1 tends to $(k'_{-1} + k_c)$ (see previous paragraph) and λ_2 $(= k_{obs}) \ll k_c$ in this pH range (Table 3). It follows that $k_c/k'_{-1} = 0.063/0.061 = 1.03\ (\pm 0.45)$, which gives an estimate for k'_{-1} based on the amplitudes of the two phases of $2.20\ (\pm 0.96) \times 10^6\ s^{-1}$. For the purpose of this study, we take the mean of the kinetic and amplitude determinations of k'_{-1}, giving $k'_{-1} = 2.10\ (\pm 1.22) \times 10^6\ s^{-1}$.

In the data at pH 7.52 and 8.04, where there is a significant fraction of $H\mathbf{A}_\mathbf{o}^+$ present at equilibrium, transients due to recovery of this species from its photochemical excitation might interfere with analysis of transients due to photolysis of $\mathbf{A}_\mathbf{c}$. For example Abs_2 (−0.073) at pH 8.04 (Fig. 4D and Table 3) would have been reduced by about 20% if the same biphasic transient arising from $H\mathbf{A}_\mathbf{o}^+$ at pH 4 (see the 'Results' Section) were present at pH 8.04. Because of this uncertainty, data at pH 7.52 and 8.04 were not used in determining k'_{-1}, although they were checked for consistency with the overall kinetic model (see below).

We briefly consider the mechanistic basis of these $40\ s^{-1}$ transients observed at pH 7.52 and 8.04 and recall that flash irradiation of the sultam at pH 4 (where it is virtually all in the $H\mathbf{A}_\mathbf{o}^+$ form) showed transients of similar form (i.e. an instantaneous absorbance decrease followed by bi-exponential recovery to the pre-flash absorbance, with the slower phase at $180\ s^{-1}$). These slow decay rates, together with previous data on near-UV laser flash illumination of rhodamines (at 532 nm and 355 nm), suggest that the species responsible for the transient decay is unlikely to be in a triplet state, since direct irradiation of rhodamines at either wavelength did not give rise to triplets.[22,23] In contrast, flash illumination of Rhodamine 123 at 355 nm has been shown to cause photoionization to a radical cation,[22] and a related process may be responsible for the transients observed here.

Returning to the extraction of rate and equilibrium constants from the experimental data, the values k'_1 and hence the pK_a of the sulfonamide were next determined using data from the pH range 8.48–10.52 where $k_{obs} \ll k_{fast}$ (Table 3). As noted above, the steady-state approximation may be applied to these data, so under this condition ($-k_{obs}t$) is equal to the exponent of Eqn (8). Furthermore, in this pH range k_{obs} is proportional to $[OH^-]$ (Table 3) and the term containing k_o may be neglected as k_o is relatively small (see below). Noting that $[H^+][OH^-] = 10^{-14.76}\ M$ (in 10 mM KCl and 4°C),[21] $k_{obs} = k'_1 k_c[OH^-]/(k'_{-1} + k_c) = 2.56\ (\pm 0.57) \times 10^9[OH^-]\ s^{-1}$. From the kinetic evaluations of k_c and $(k'_{-1} + k_c)$ described above, $k'_1 = 4.8\ (\pm 2.0) \times 10^9\ M^{-1}\ s^{-1}$. From this value of k'_1 and that of k'_{-1} $[2.10\ (\pm 1.22) \times 10^6\ s^{-1}]$, the kinetically determined pK_a for the sulfonamide is 11.40.

The photochemical data contain anomalies and these need to be addressed. Rate constants and amplitudes at pH 10.99 and 11.50 are not as predicted. At pH 10.99 predicted values from Eqns (4), (5), and (7) of λ_1, λ_2, and Abs_1/Abs_2 are $6.0 \times 10^6\ s^{-1}$, $4.0 \times 10^5\ s^{-1}$, and 0.50, respectively, and at pH 11.50 are $7.5 \times 10^6\ s^{-1}$, $0.85 \times 10^6\ s^{-1}$, and 0.27. Calculations of early signal loss (shown in 'Experimental' Section) suggest 73% and 77% loss of the fast phases at pH 10.99 and 11.50, respectively. Furthermore, the increased amplitudes of the k_{slow} phase at these pH values compared to those at pH 12.50 and 13.05 (Table 3) suggest this transient of unknown origin has a

component due to a putative λ_2-transient. It is not surprising that data analysis of the λ_1- and λ_2-transients, distorted at short times by loss of signal and at long times by the transient of unknown origin, gives rise to anomalies. Simulations (not shown) incorporating anomalous transients (e.g. those in Fig. 4C and its insert) supported the view that inconsistency of the pH 10.99 and 11.50 data with the Scheme 2 model was for the above reasons and not because of failure of the model. The same calculations at pH 11.99 give λ_1, λ_2, and Abs_1/Abs_2 values of $1.22 \times 10^7\,s^{-1}$, $1.96 \times 10^6\,s^{-1}$, and 0.03. As expected the most rapid phase is not observed. The major process predicted to occur at $1.96 \times 10^6\,s^{-1}$ is close to k_{obs} of $2.21 \times 10^6\,s^{-1}$ (Table 3).

In contrast to data from the photochemical experiments, the stopped-flow data were obtained at acidic to neutral pH and led to determination of values for further rate and equilibrium constants shown in Scheme 3. However, there was some pH overlap and it is noteworthy that the k_{obs} value measured by stopped-flow at pH 7.36 ($245\,s^{-1}$, Table 1) is close to that measured photochemically at pH 7.52 ($297\,s^{-1}$, Table 3). As expected, k_{obs} values in the stopped-flow experiments near pH 7 (MOPS buffer, Table 1) were equal (within the sum of the SD values), whether the equilibrium was approached from acidic (predominantly $H\mathbf{A_o^+}$) or basic (predominantly $\mathbf{A_c}$) conditions.

Values of k_{obs} above pH 5.5 in Table 1 equate to $(k'_1k_c[OH^-] + k'_{-1}k_o)/(k'_{-1} + k_c)$ (from Eqn (8)). The photochemical data, as discussed above, showed that the first term of this expression, $k'_1k_c[OH^-]/(k'_{-1} + k_c) = 2.56\ (\pm 0.57) \times 10^9[OH^-]\,s^{-1}$. The contribution of this term to k_{obs} is negligible below pH 5.5 but equal to 1.6, 5.7, 17, 30, 48, and $102\,s^{-1}$ in data at the respective pH values between 5.56 and 7.36 listed in Table 1. These values were subtracted from the appropriate k_{obs} to leave a data set for k_{obs}' (Table 1) to be equated with $k'_{-1}k_o/(k'_{-1} + k_c)$.

When solutions containing **4** are changed rapidly from initial pH 9 to values in the pH range 2–5, the rate of formation of $H\mathbf{A_o^+}$ depends strongly on pH, with an order of magnitude decrease between pH 2.55 and 2.14 (Table 1). When the pH is lowered, the first process is evidently a rapid equilibration between $H_2\mathbf{A_c^{2+}}$, $H\mathbf{A_c^+}$, and $\mathbf{A_c}$, which is followed by ring opening to form $H\mathbf{A_o^+}$ in a flux through $\mathbf{A_c}$ and $\mathbf{A_o}$. The decrease in rate occurs because ring opening can only occur through $\mathbf{A_c}$, whose concentration has been reduced by its rapid protonation. Calculation of the flux through $\mathbf{A_c}$ requires estimates of $pK_{H\mathbf{A_c}}$ and $pK_{\mathbf{A_c}}$, the pK_a values of the tertiary amino groups in $\mathbf{A_c}$. Thus the flux decreases by the factor $\{1 + ([H^+]/K_{\mathbf{A_c}})(1 + [H^+]/K_{H\mathbf{A_c}})\}$. The exponent in Eqn (8) has to be modified to accommodate this reduced flux, leading to Eqn (13) as:

$$k'_{obs} = \frac{k'_{-1}k_o}{(k'_{-1} + k_c)}\left\{1 + \left(\frac{[H^+]}{K_{\mathbf{A_c}}}\right)\left(\frac{1 + [H^+]}{K_{H\mathbf{A_c}}}\right)\right\} \qquad (13)$$

Combining all the stopped-flow data in a least-squares fit to Eqn (13) gave values for $k'_{-1}k_o/(k'_{-1} + k_c)$, $pK_{H\mathbf{A_c}}$ and $pK_{\mathbf{A_c}}$ of 142 (± 7)$\,s^{-1}$, 3.24 (± 0.08) and 4.72 (± 0.06), respectively. Since $k_c/(k'_{-1} + k_c) = 0.53$ (± 0.21), it follows that $k'_{-1}/(k'_{-1} + k_c) = 0.47$ (± 0.19) and $k_o = 302$ (± 137)$\,s^{-1}$. To maintain thermodynamic balance the sum of $pK_{H\mathbf{A_c}}$ and $pK_{\mathbf{A_c}}$ (i.e. 7.96) must equal the sum (8.05) of the two apparent pK_a values associated with the color changes (absorbance data in Fig. 2), namely $H\mathbf{A_o^+}$ to $\mathbf{A_c}$ (7.37) and $H_2\mathbf{A_c^{2+}}$ to $H\mathbf{A_o^+}$ (0.68). Given the different analytical methods and the uncertainty of pH measurement at high acidity, the agreement is satisfactory. Furthermore, the derived values for $pK_{H\mathbf{A_c}}$ and $pK_{\mathbf{A_c}}$ are similar to the corresponding pK_a values of 2.97 and 4.52 previously determined for lactam **8** by spectrophotometric titration.[7]

The kinetic data (Table 2) when solutions of $H\mathbf{A_o^+}$ are acidified to low pH and form $H_2\mathbf{A_c^{2+}}$ show that the reaction is H^+-dependent. Before processing these data it was useful to subtract contributions to k_{obs} from the OH^--dependent pathway (i.e. via Eqn (9)). These contributions were calculated from Eqn (13) for the four data points at pH values from 0.0 to 1.0, giving k_{obs}' values of 1.6×10^{-6}, 6.2×10^{-6}, 3.9×10^{-5}, and $1.6 \times 10^{-4}\,s^{-1}$ at the respective pH values of Table 2 and subtraction of these from k_{obs} gave k^*_{obs} (Table 2). To analyze the data in terms of Eqn (10) we assume that all species between $\mathbf{A_o}$ and $H_2\mathbf{A_c^{2+}}$ are in equilibrium during the reaction. In the pH range of 0–1 it then follows that $[\mathbf{A_o}]/[H_2\mathbf{A_c^{2+}}] = k_oK_{\mathbf{A_c}}K_{H\mathbf{A_c}}/k_c[H^+]^2$. Since the only species present at significant concentration are $H\mathbf{A_o^+}$ and $H_2\mathbf{A_c^{2+}}$, the observed process is a single exponential decay of $H\mathbf{A_o^+}$ to an equilibrium mixture of $H\mathbf{A_o^+}$ and $H_2\mathbf{A_c^{2+}}$ in which $k^*_{obs} = k^*_1 + k^*_{-1}[H^+][\mathbf{A_o}]/[H_2\mathbf{A_c^{2+}}]$. Substituting $[\mathbf{A_o}]/[H_2\mathbf{A_c^{2+}}]$ gives Eqn (14):

$$k^*_{obs} = k^*_1 + \frac{k^*_{-1}k_oK_{\mathbf{A_c}}K_{H\mathbf{A_c}}}{k_c[H^+]} \qquad (14)$$

However, this equation implies that k^*_{obs} will decrease with increasing $[H^+]$, contrary to what is observed, so ruling out Eqn (10) as being part of the reaction pathway. Accordingly, it is likely that an alternate route from $H\mathbf{A_o^+}$ to $H_2\mathbf{A_c^{2+}}$ exists, possibly a direct pathway as shown in Scheme 3 controlled by k_A and k_{-A}. The data at each pH in Table 2 were therefore analyzed according to Eqn (15), and using the pK_a value of 0.68 for the transformation (Fig. 2). Values of k_A and k_{-A} were then averaged to give values ($\pm$SD) listed in Table 4.

$$k^*_{obs} = k_A[H^+] + k_{-A} \qquad (15)$$

Data described in the supplementary information show that the spectrum of the protonated species recorded in 2 M HCl was very similar to that previously described[7] for the doubly protonated form of the lactam **8**, that is consistent with its formulation as $H_2\mathbf{A_c^{2+}}$. However, the precise details of the transition from $H\mathbf{A_o^+}$ to $H_2\mathbf{A_c^{2+}}$ remain unclear. What is surprising is that, as described in the 'Results' Section, Sulforhodamine B undergoes rapid protonation to a species which has the open structure **9** on the basis of previous data,[9–12] whereas sultam **4** undergoes slow conversion to the closed, doubly protonated form $H_2\mathbf{A_c^{2+}}$. Absorption spectra recorded during the slow decolorization showed no evidence of a protonated intermediate

Table 4. Rate and equilibrium constants ($\pm$SD) used in Eqn (16)

Derived constant	Value
$10^{-2}k_o$ (s^{-1})	3.02 ($\pm$1.37)
$10^{-6}k_c$ (s^{-1})	2.27 ($\pm$0.08)
10^3k_A ($M^{-1}\,s^{-1}$)	1.4 ($\pm$0.4)
10^4k_{-A} (s^{-1})	2.9 ($\pm$0.8)
$10^{-9}k'_1$ ($M^{-1}\,s^{-1}$)	4.8 ($\pm$2.0)
$10^{-6}k'_{-1}$ (s^{-1})	2.10 ($\pm$1.22)
$pK_{H\mathbf{A_c}}$	3.24 ($\pm$0.08)
$pK_{\mathbf{A_c}}$	4.72 ($\pm$0.06)

Journal of Physical Organic Chemistry

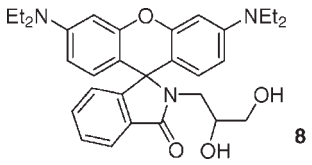

8

Figure 7. Structure of compound **8**

equivalent to the open form **9**. It is implicit in these data that protonation of $H\mathbf{A}_o^+$ is a slow step followed by rapid cyclization to $H_2\mathbf{A}_c^{2+}$. One rationalization of the different behavior of Sulforhodamine B and sultam **4** upon exposure to strong acid is that the sulforhodamine (net overall single negative charge) undergoes rapid protonation, whereas the sultam, which as $H\mathbf{A}_o^+$ bears no net charge, is protonated to an open dication analogous to **9** much more slowly and that the dication is then rapidly quenched by internal attack of the sulfonamido group.

Using the set of rate and equilibrium constants derived above and summarized in Table 4, we can calculate a plot of the overall rate constant against pH, k_{calc} (see below) that is compared in Fig. 9 with the combined k_{obs} data set from Tables 1–3. k_{calc} was calculated (Eqn (16)) for data in the pH range of 0–10.52.

$$k_{calc} = k_A[H^+] + k_{-A} + \frac{k_o k'_{-1}}{(k'_{-1} + k_c)\{1 + ([H^+]/K_{\mathbf{A_c}})(1 + [H^+]/K_{H\mathbf{A_c}})\}} + \frac{k'_1 k_c [OH^-]}{k'_{-1} + k_c} \quad (16)$$

For data from pH 11.99 to 13.05, k_{calc} was taken as equal to k_c. No estimate of k_{calc} was made at pH 10.99 and 11.50 because the data were influenced by factors discussed above.

The predicted ratio $[H\mathbf{A}_o^+]/[\mathbf{A}_T]$, where $[\mathbf{A}_T]$ is the total concentration of **4**, was also tested as a function of pH (Eqn (17)) from 567 nm absorption measurements in the pH range of 0–10 (Fig. 2). Since $[H^+][\mathbf{A_c}]/([H\mathbf{A}_o^+] + [\mathbf{A_o}]) = 10^{-7.37}$ M and the concentration of $\mathbf{A_o}$ is negligible below pH 10.

$$\frac{[H\mathbf{A}_o^+]}{[\mathbf{A}_T]} = \left(1 + \frac{10^{-7.37}\{1 + ([H^+]/K_{\mathbf{A_c}})(1 + [H^+]/K_{H\mathbf{A_c}})\}}{[H^+]}\right)^{-1} \quad (17)$$

Both the equilibrium and kinetic data sets in Figs 2 and 9, respectively, fit theory as formulated by Eqns (16) and (17) well, as judged by eye. The principal exception is for the data points of Fig. 2 at the lowest pH values. This deviation is discussed in the 'Results' Section and Figure S1 of the Supplementary Information. A more objective estimate of the kinetic agreement is given by

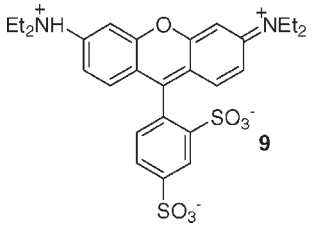

9

Figure 8. Structure of compound **9**, which corresponds to a protonated form of compound **1**

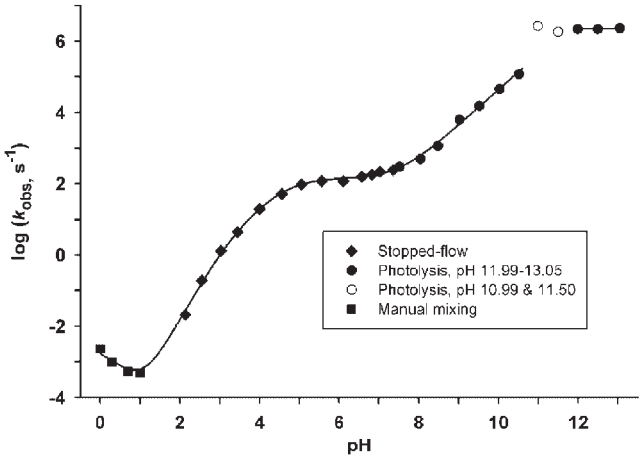

Figure 9. Dependence of k_{calc} on pH for sultam **4**. Values of k_{obs} are plotted from data in Tables 1–3 acquired using stopped-flow, manual mixing, and laser-pulse photolysis. The line is a plot of the logarithm of the calculated rate constant (k_{calc} of Eqn (16)) against pH for the pH range 0.0–10.52, using the rate and equilibrium constants listed in Table 4, and against pH for the range 11.99–13.05 using k_c. No line is drawn through the anomalous data points at pH 10.99 and 11.50 (as discussed in the text)

determining the extent to which individual data points lie within the SD range of k_{calc} as defined by Eqn (16), that is from pH 0.0 to 10.52. These SD values were calculated from Eqn (16) using those of k_A, k_{-A}, $pK_{\mathbf{A_c}}$, and $pK_{H\mathbf{A_c}}$ (from Table 4) and of $k_o k'_{-1}/(k'_{-1} + k_c)$ and of $k'_1 k_c/(k'_{-1} + k_c)$ (see text above). Fifteen of the 24 data points in the pH range 0.0–10.52 lie within one SD of k_{calc} at the relevant pH value. For the subset of stopped-flow data, 8 of the 13 data points are within one SD of the k_{calc} values. If the spread of the data points is described by a Gaussian distribution, then 68% of the data points (i.e. 16 and 9, respectively, for the whole pH range 0.0–10.52 and for the stopped-flow data) should lie within the 1 SD limits. Thus Scheme 3 and its associated equilibrium and rate constants provide a quantitative description of the data. Finally, the absorption spectrum of **4** measured at pH 12 showed that at equilibrium, the residual absorption (shown in 'Results' Section) corresponded to ~0.014% of the total rhodamine being present as $\mathbf{A_o}$. This agrees well with the predicted value for the $[\mathbf{A_o}]/[\mathbf{A_c}]$ ratio of 1.34×10^{-4} (i.e. from k_o/k_c).

Thus, the kinetic and equilibrium data over a 3×10^{12}-fold range of H^+ concentration provide a relatively stringent test of Scheme 3. The presence of ethanol in the solvent may affect the water ionic-product value of $10^{-14.76}$ M,[21] but error in the ionic-product value will only cause error in k'_1 amongst the constants in Table 4, since the only appearance of $[OH^-]$ in the equations is as a product with k'_1.

The mechanism derived above contains several points of interest. First, the pK_a of 11.40 derived for $H\mathbf{A}_o^+$ from the kinetic results is compatible with known data (e.g. *N*-methylbenzenesulfonamide has pK_a 11.43).[20] It is noteworthy, though not unexpected, that the bimolecular rate constant of 4.8 (±2.0) × 10^9 M^{-1} s^{-1} at 4°C determined here for reaction of hydroxide ion with the sulfonamide proton is comparable with related diffusion-controlled processes.[5] While at low pH there is evidence for H^+-dependent protonation of $H\mathbf{A}_o^+$ with a rate constant of 1.4 (±0.4) × 10^{-3} M^{-1} s^{-1}, there is no evidence for a kinetically competent protonation of $\mathbf{A_o}$ (Eqn (10)). This is

expected for ionizable compounds whose pK_a values are far removed from 7.[5]

The mechanism as described implies facile unimolecular fission of the elongated endocyclic C—N bond of the sultam, with the arylsulfonamide anion as the leaving group, yet there is little precedent for such a reaction. Ring opening of *N*-arenesulfonylaziridines under neutral conditions appears to be one such analogue, although in that case ring strain is a major influence on the reactivity.[24] The pH-independent hydrolysis of the amide group in the *N*-benzoylsultam **10** is a related example, although the base-catalyzed rate is dominant, even at neutral pH.[25] The anomalous acylation of a serine residue in elastase by the oxosultam **11** that involves ring-opening with C—N cleavage is another example,[26] although both reactions are likely initiated by attack of an external nucleophile on the relevant carbonyl group. In the present case, C—N bond cleavage in the rhodamine sultam must be driven by the stability of the highly delocalized cation that is formed. The cleavage would be facilitated by the relative weakness of the endocyclic C—N bond, that is 0.06 Å longer than its exocyclic companion. In the latter context, it is noteworthy that the scissile C—O bond in several members of the well-known family of photochromic spirooxazines[27] has also been shown to be longer (by 0.03–0.05 Å) than typical C—O bonds in related oxygen heterocycles (Fig. 10).[28–30]

A related C—N heterolysis process occurs in the hydrolysis of tritylamines, where a less marked extension (0.02 Å) of the labile C—N bond has been noted.[31] Kinetic studies of the acidic hydrolysis of di- and tri(*p*-methoxy)tritylamine[32,33] suggest that the protonated amine undergoes C—N bond cleavage to give an ion-molecule complex [Ar_3C^{+} $^{\bullet}NR_3$], that converts to products via both spontaneous and acid-catalyzed paths. The spontaneous reaction is an S_N1-like process in which the nucleofuge is an amine. Ring opening for the rhodamine sultam **4** ($\mathbf{A_c} \rightarrow \mathbf{A_o}$) is similar except that the leaving group is a sulfonamide anion. For tritylamines the partition between acid-catalyzed and uncatalyzed pathways varied considerably as substituents on the aryl groups and amine changed[33] and the kinetic parameters of Scheme 3 would doubtless show some variations if differently substituted sultams were considered.

Half-times for decay of the photochemically generated open form of **4** are in the μs time domain, in marked contrast with the value of 1.7 s reported for a similar sultam in acetonitrile solution.[13,14] Furthermore, half-times of ~300 s were reported[13,14] for comparable experiments on lactams similar to **8**. No explanation was offered as to factors that might cause these zwitterionic structures to persist for such extended times in a relatively non-polar solvent. Given the present results, it seems likely that the photochemically generated zwitterion in those experiments (corresponding to the species $\mathbf{A_o}$) underwent rapid *N*-protonation by trace hydroxylic contaminants in the solvent. The observed decay of the rhodamine chromophore could then be understood in terms of slow reversal of this protonation to allow reclosure of the sultam or lactam. Slower recyclization of the amide can be rationalized on the grounds of the lower acidity of the amide proton.

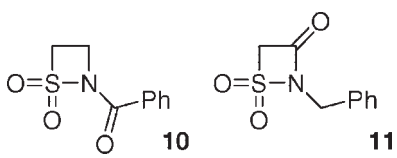

Figure 10. Structures of compounds **10** and **11**

It is surprising that lactam derivatives of carborhodamines such as **8** do not show pH-dependent behavior similar to that of sultams, although the mechanism shown in Scheme 3 allows the resistance to ring opening to be understood in terms of better stabilization of a sulfonamide anion than an amide anion. This stability of the closed form may be of benefit in future applications, since these lactams are also known to undergo photochemical ring opening and, as indicated above, the kinetics of the reclosure in aqueous solution are expected to be much faster than in aprotic organic solvents.[13,14] Thus both the sultams and lactams appear to have the capacity to act as transient chromophores and fluorophores on the μs—ms time scale. Possible applications as transient reporter groups, especially as orientation probes within biological systems, are under consideration.

While this work was in review, we became aware of a related recent study, in which photochemical opening of a rhodamine B lactam (i.e. a structure related to that of compound **8** herein) was used in several imaging applications.[34] Only qualitative data about the persistence of the open form in different solution conditions were made [i.e. hours in organic (PVA) or milliseconds in unspecified polar solvents] but the revival of interest in these compounds following the earlier work by the Gleiter group[13,14] demonstrates the relevance of an understanding of the interconversion between colored and colorless forms of these dyes.

EXPERIMENTAL

General

The mixture of **4** and **5** (~2.6:1 ratio) was prepared and used for isolation of pure **4** as described previously.[7] The bis-pyrrolidinyl sulforhodamine **6** was available from previous work.[15] Silica gel for flash chromatography was Merck type 9385. Elemental analysis was by MEDAC Ltd, Egham, UK Aqueous solutions of Sulforhodamine B derivatives were quantified by visible spectroscopy at 567 nm based on the absorption coefficient of 114 000 M^{-1} cm^{-1} determined for sulforhodamine **6** in aqueous solution.[15] Concentrations of total rhodamine in pH-dependent species were estimated from the absorbance of solutions at pH 4. Buffer solutions for all spectroscopic and kinetic measurements were prepared from solutions in water—EtOH (3:1 v/v) of appropriate acids at the molarities specified and adjusted to the required pH values by addition of NaOH. pH-values were determined with a glass electrode referenced to buffer solutions in 100% aqueous solution. As noted in the 'Introduction', little perturbation of measured pH values is expected at this level of ethanol content.[8]

3′,6′-Di(1-pyrrolidinyl)-2-methylspiro[1,2-benzisothiazole-3(2H),9′-[9H]xanthene]-1,1-dioxide (7)

A suspension of sulforhodamine **6** (178 mg, 0.375 mmol) in $POCl_3$ (2.5 ml) was kept for 18 h at room temperature, during which time the mixture first solidified (~1 h), and then turned slowly to a homogeneous liquid. This was diluted with $CHCl_3$ (~150 ml) and washed with ice-cold water and ice-cold 10% aq. $NaHCO_3$, then shaken vigorously with cold 40% aq. methylamine (40 ml). The $CHCl_3$ solution was washed with water, 1 M HCl, and 10%

$NaHCO_3$, dried and the solvent was removed. Flash chromatography (EtOAc–hexanes 3:7) followed by crystallization (benzene–hexanes) gave **7** as colorless needles (156 mg, 69%), mp 292–294°C (dec) UV (EtOH): λ_{max} (EtOH)/nm (ε/M^{-1} cm^{-1}) 274 sh (22 900) and 310 (15 600); ^{1}H NMR (400 MHz, $CDCl_3$) δ 7.88 (1 H, dd, $J = 7.2$ and 1.5 Hz, H-7), 7.40–7.48 (2 H, m, Ar—H), 7.36 (9 H, s, 1.5 benzene of solvation), 7.00 (1 H, dd, $J = 7.0$ and 1.5 Hz, H-4), 6.92 (2 H, d, $J = 9.3$ Hz, H-1′, 8′), 6.29 (2 H, d, $J = 1.5$ Hz, H-4′, 5′), 6.27 (2 H, dd, $J = 9.3$ and 1.5 Hz, H-2′, 7′), 3.27–3.30 (8 H, m, NCH_2), 2.49 (3 H, s, Me), and 1.98–2.02 (8 H, m, CH_2). Anal. calculated for $C_{28}H_{29}N_3O_3S \cdot 1.5\ C_6H_6$: C, 73.48; H, 6.33; N, 6.95. Found: C, 73.16; H, 6.16; N, 6.99.

Kinetic measurements

Stopped-flow measurements were made at 4°C using a HiTech MX51 instrument (TgK Scientific, Bradford-on-Avon, UK) operated in single-push mode, with a 10% pre-trigger and mixing of equal volumes of the two solutions in each run. Light from a quartz halide lamp was passed through a monochromator set to 567 nm and observed through a 1 cm path length. Transmission data were converted to absorbance and analyzed as the best fit to single exponentials using the HiTech software. All buffer solutions were prepared in water−EtOH (3:1 v/v) as described above. For stopped-flow measurements going from high to low pH, the **4** plus **5** mixture was diluted to 9 μM (i.e. 6.5 μM **4**, 2.5 μM **5**) in 5 mM Na borate, pH 9.0 and for measurements in the opposite direction it was diluted in 5 mM Na citrate, pH 4.0. Mixing buffers (100 mM) contained citrate (pH 2.0–6.0), 2-(*N*-morpholino) ethanesulfonate (MES, pH 6.5), or 3-(*N*-morpholino)propanesulfonate (MOPS, pH 7.0 and 7.5).

Kinetic experiments at high [H^+] were performed at 4°C in a Beckman DU640 spectrophotometer. Equal volumes of HCl (0.2–2 M) and a solution of 7.0 μM **4** (and 2.7 μM **5**) in 1 mM HCl, each in water–EtOH (3:1 v/v) and pre-cooled to 4°C, were mixed by hand (~30 s) and absorbance at 567 nm was monitored. Data were transferred to Microsoft Excel™ and analyzed as single exponentials.

Solutions of **4** (21 μM) for pulse-laser photochemistry were prepared similarly to those for the stopped-flow experiments, but with 55 mM buffer concentrations for comparability with the post-mixing concentrations in those experiments. Solutions were prepared from *N*-(2-hydroxyethyl)piperazine-*N*′-3-propanesulfonate (EPPS, pH 8.0 and 8.5), 2-(cyclohexylamino)ethanesulfonic acid (CHES, pH 9.0 and 9.5), 3-(cyclohexylamino)propanesulfonic acid (CAPS, pH 10–11). Above pH 11, solutions of NaCl (pH 11.50, 97 mM; pH 11.99, 90 mM; pH 12.50, 68 mM; pH 13.05, 0 mM) were adjusted to the required pH values with 1 M NaOH. Solutions were irradiated at 4°C in a quartz cell (path length 10 mm) using a Lambda Physik LPX 100 XeCl excimer laser producing 30 ns 150 mJ pulses at 308 nm and focused with two orthogonally set cylindrical lenses. Typically, 10 records were averaged using a Luzchem model LFP-111 transient recorder and Tektronix digitizer (300 MHz bandwidth). Recording was initially at 567 nm but later experiments were recorded at 547 nm to minimize interference in the first ~100 ns after the light flash. Most kinetic data were fitted to two exponentials, but for the fastest time sweeps (4 μs full-scale) only a small proportion of the second exponential was present and the fit was to a single exponential plus a straight line. To minimize interference from the laser flash in the 4 μs full-scale time sweeps, the data were processed using a built-in instrument correction that partially attenuated the magnitude of this perturbation. Prior to the 10-record averaging, each record had a partner in which the monitor beam was shuttered (i.e. only scattered light/fluorescence was detected) that was subtracted from the raw data. The resultant averaged 10-record data set then had a corresponding data set from a blank solution subtracted from it. All fits were made using unweighted non-linear routines in Microsoft Excel™. Abs_1 values (Table 3) had two components. The first component was measured from the time at which the absorption peaked (i.e. time zero on the abscissa as in Fig. 4B). To this was added the 0.015 absorbance calculated by taking into account the mean interval of 64 ns between the time of the maximum intensity of the laser pulse and time zero. Abs_2 values in the pH range 8.48–13.05 (Table 3) were calculated by subtracting the Abs_1 amplitudes from the overall amplitudes.

Error ranges are recorded as SD of individual experimental trials (e.g. Table 1), accumulated data sets (e.g. pK_{HA_c} and pK_{A_c}) or by combining SD of two measurements to calculate the SD of a third entity using standard procedures for propagation of errors[35] [e.g. k_{-1} from k_c and $(k_{-1} + k_c)$].

Spectroscopic pH titration and related measurements

A stock solution of **4** (1 mM in aq. MeOH) was diluted to 8.3 μM in aq. ethanol solutions of 25 mM buffers (citrate, MES, MOPS, EPPS, CHES, and CAPS over the pH range of 2–10 as described above) or 0.2–1 M HCl. Solutions were kept at room temperature for 2 h to ensure equilibration of **4** at low pH and their absorption at 567 nm was measured.

For the measurement at high pH, the same stock solution of **4** was diluted to 84 μM in 90 mM NaCl adjusted to pH 12 (also in aq. ethanol as for the kinetic measurements) and its absorbance spectrum was measured. The absorbance at the maximum value (~555 nm) was manually corrected for the sloping baseline absorbance and the concentration of open rhodamine was calculated. The total 555 nm absorbance (1 cm path length) was ~0.004 and the baseline-corrected value was ~0.0016, corresponding to ~14 nM open rhodamine, that is 0.016% of the total rhodamine concentration.

The UV spectrum of the closed form of **4** was measured in aq. ethanolic CAPS, pH 10.5. The absorption coefficient at 308 nm (the wavelength of the excimer laser used above) was 15 300 M^{-1} cm^{-1}.

Crystallographic details for sultam (7)

Crystals were grown from chloroform–ethanol solution. A single crystal *ca.* 0.05 × 0.05 × 0.1 mm^3 mounted on a glass fiber was used for crystallographic measurements. Intensity data were collected at 20°C using a 30-cm MAR imaging plate on beamline BW7A at the EMBL outstation, Hamburg, Germany using monochromatic radiation of wavelength 0.748 Å. Two data sets with different crystal-to-detector distances, exposure times, and oscillation ranges were merged to give a final data set 92% complete from 10 Å to 0.83 Å. Data were processed and reduced using DENZO and SCALEPACK, respectively.[36] The structure was solved by direct methods (SHELXS-86).[37] Refinement was carried out using intensities, F^2, in SHELX97.[38] Anisotropic temperature factor refinement was carried out on all non-hydrogen atoms and all hydrogen atoms were refined using a rigid model (C_{sp2}-H = 0.93 Å, C_{sp3}-H = 0.96 Å with $U_{iso}(H[C_{sp2}]) = 1.2U_{eq}(C_{sp2})$, $U_{iso}(H[C_{sp2}]) = 1.2U_{eq}(C_{sp2})$, and $U_{iso}(H[C_{sp3}] = 1.5U_{eq}(C_{sp3}))$.

Full-matrix least squares refinement of 318 parameters for 4097 independent reflections [$I \geq \sigma(I)$] gave $R_F = 0.0865$ and $wR_I = 0.2259$ ($R_F = 0.0538$ and $wR_I = 0.1814$ on 2748 $I \geq 2\sigma(I)$ data). The atomic coordinates are given in the Supplementary Information as a cif file.

Supporting Information Available

Low pH titration and spectroscopic data for the sultam **4** (pdf), and a table of atomic coordinates for the crystal structure of the sultam **7** (cif). This material is available via the Internet on the Wiley InterScience website.

Acknowledgements

We thank Dr V. R. N. Munasinghe for recording NMR spectra, and Drs Z. Dauter and S. R. Martin for their help with crystallographic data collection and kinetic data analysis, respectively. We are grateful to the MRC Biomedical NMR Center for access to facilities. The York Structural Biology Laboratory is funded by the BBSRC.

REFERENCES

[1] J. E. T. Corrie, B. D. Brandmeier, R. E. Ferguson, D. R. Trentham, J. Kendrick-Jones, S. C. Hopkins, U. A. van der Heide, Y. E. Goldman, C. Sabido-David, R. E. Dale, S. Criddle, M. Irving, *Nature* **1999**, *400*, 425–430.
[2] R. E. Ferguson, Y. B. Sun, P. Mercier, A. S. Brack, B. D. Sykes, J. E. T. Corrie, D. R. Trentham, M. Irving, *Mol. Cell* **2003**, *11*, 865–874.
[3] J. N. Forkey, M. E. Quinlan, M. A. Shaw, J. E. T. Corrie, Y. E. Goldman, *Nature* **2003**, *422*, 399–404.
[4] A. Yildiz, J. N. Forkey, S. A. McKinney, T. Ha, Y. E. Goldman, P. R. Selvin, *Science* **2003**, *300*, 2061–2065.
[5] M. Eigen, *Angew. Chem. Int. Edn. Engl.* **1964**, *3*, 1–19.
[6] O. F. Mohammed, D. Pines, E. T. J. Nibbering, E. Pines, *Angew. Chem. Int. Edn. Engl.* **2007**, *46*, 1458–1461.
[7] J. E. T. Corrie, C. T. Davis, J. F. Eccleston, *Bioconjug. Chem.* **2001**, *12*, 186–194.
[8] R. G. Bates, *Determination of pH. Theory and Practice*, Wiley, New York, **1964**. 201–229.
[9] R. W. Ramette, E. B. Sandell, *J. Am. Chem. Soc.* **1956**, *78*, 4872–4878.
[10] N. O. Mchedlov-Petrossyan, *Russ. J. Phys. Chem.* **1981**, *55*, 976–978.
[11] N. B. Zorov, A. P. Golovina, I. P. Alimarin, Z. M. Khvatkova, *Russ. J. Anal. Chem.* **1971**, *26*, 1466–1470.
[12] N. O. Mchedlov-Petrossyan, S. A. Shapovalov, S. I. Egorova, V. N. Kleshchevnikova, E. Arias Cordova, *Dyes Pigm.* **1995**, *28*, 7–18.
[13] K. H. Knauer, R. Gleiter, *Angew. Chem. Int. Edn. Engl.* **1977**, *16*, 113.
[14] H. Willwohl, J. Wolfrum, R. Gleiter, *Laser Chem.* **1989**, *10*, 63–672.
[15] L. Cavallo, M. H. Moore, J. E. T. Corrie, F. Fraternali, *J. Phys. Chem. A* **2004**, *108*, 7744–7751.
[16] T. M. Lowry, W. T. John, *J. Chem. Soc.* **1910**, *97*, 2634–2645.
[17] J. W. Moore, R. J. Pearson, *Kinetics and Mechanism*, 3rd ed., Wiley, New York, **1981**. 284–333.
[18] K. Török, D. R. Trentham, *Biochemistry* **1994**, *33*, 12807–12820.
[19] P. Atkins, J. de Paula, *Atkins' Physical Chemistry*, 7th ed., Oxford University Press, Oxford, **2002**. 885–886.
[20] J. F. King, In *The Chemistry of Sulphonic Acids, Esters and Their Derivatives* (Eds: S. Patai, Z. Rappoport), Wiley, Chichester, **1991**. 249–259.
[21] H. S. Harned, W. J. Hamer, *J. Am. Chem. Soc.* **1933**, *55*, 2194–2206.
[22] M. W. Ferguson, P. C. Beaumont, S. E. Jones, S. Navaratnam, B. J. Parsons, *Phys. Chem. Chem. Phys.* **1999**, *1*, 261–268.
[23] P. C. Beaumont, D. G. Johnson, B. J. Parsons, *J. Photochem. Photobiol. A* **1997**, *107*, 175–183.
[24] B. Bucholz, H. Stamm, *Isr. J. Chem.* **1986**, *27*, 17–23.
[25] N. Ahmed, W. Y. Tsang, M. I. Page, *Org. Lett.* **2003**, *6*, 201–203.
[26] W. Y. Tsang, N. Ahmed, L. P. Harding, K. Hemming, A. P. Laws, M. I. Page, *J. Am. Chem. Soc.* **2005**, *127*, 8946–8947.
[27] S. Maeda, In *Organic Photochromic and Thermochromic Compounds*, *Vol. 1* (Eds: J. C. Crano, R. J. Guglielmetti), Plenum, New York, **1999**. 85–107.
[28] W. Clegg, N. C. Norman, J. G. Lasch, W. S. Kwok, *Acta Cryst.* **1987**, *C43*, 804–806.
[29] W. Clegg, N. C. Norman, T. Flood, L. Sallans, W. S. Kwok, P. L. Kwiatkowski, J. G. Lasch, *Acta Cryst.* **1991**, *C47*, 817–824.
[30] Y. T. Osano, K. Mitsuhashi, S. Maeda, T. Matsuzaki, *Acta Cryst.* **1991**, *C47*, 2137–2141.
[31] A. P. Henderson, J. Riseborough, C. Bleasdale, W. Clegg, M. R. J. Elsegood, B. T. Golding, *J. Chem. Soc. Perkin Trans. 1*, **1997**, 3407–3414.
[32] C. Bleasdale, B. T. Golding, W. H. Lee, H. Maskill, J. Riseborough, E. Smits, *J. Chem. Soc. Chem. Commun.* **1994**, 93–94.
[33] M. C. López, J. C. Martinez, I. Demirtas, H. Maskill, E. Stix, *Org. Reactivity* **1997**, *31*, 71–77.
[34] J. Fölling, V. Belov, R. Kunetsky, R. Medda, A. Schönle, A. Egner, C. Eggeling, M. Bossi, S. W. Hell, *Angew. Chem. Int. Edn. Engl.* **2007**, *46*, 6226–6270.
[35] J. R. Taylor, In *An Introduction to Error Analysis*, 2nd ed., University Science Books, Sausalito, **1997**, 45–91.
[36] Z. Otwinowski, W. Minor, *Methods Enzymol.* **1997**, *276*, 307–326.
[37] G. M. Sheldrick, *Acta Cryst.* **1990**, *A46*, 467–473.
[38] G. M. Sheldrick, *SHELXL97, Program for Refinement of Crystal Structures*, University of Göttingen, Germany, **1997**.